Indian J. Met. Hydrol. Geophys. (1978), **29**, 1 & 2, 170-186

551·553·21 : 551·51(3215-77)

*Temporal variations in the northern hemispheric summer circulations**

MANAKKAMPAD S. UNNINAYAR and TAKIO MURAKAMI

Department of Meteorology, University of Hawaii, Honolulu, Hawaii

ABSTRACT. Changes in kinetic energy averaged over the tropical (5·0°S-19·6°N), subtropical (24·2°N-37·1°N) and mid-latitude (41·0°N-48.1°N) belts were examined for the 92-day period from June through August 1970. Somewhat systematic fluctuations (10-15 day period) were observed in the eddy and zonal mean kinetic energies of the 200 mb tropical belt. Mid-latitude periodicity was longer at about 20 days. Short period (~5 day) fluctuations were considerably stronger at 700 mb than that at 200 mb, over the tropical belt.

Abnormal transitions were observed to begin around 12 July with a simultaneous decrease in 200 mb eddy kinetic energy at all latitudes, 700 mb eddy kinetic energy over the tropical belt, and tropical baroclinic activity as determined from cloudiness; all reached minimum values around 20-24 July. On the other hand, tropical zonal mean kinetic energy increased to maximum values in the same period.

During 20-24 July, the tropospheric circulation displayed singularly different characteristics compared to normal, and "break monsoon" conditions prevailed over India. The zones of cloudiness and upper divergence maxima over the monsoon region shifted northwards to the Tibetan area, while dry weather and abnormal upper convergent wind inflow was experienced over southeast Asia. A conspicuous and anomalous excitation of convective activity over tropical regions in the western North and South Pacific was associated with pronounced upper (lower) tropospheric anticyclonic (cyclonic) circulations. Consequently, 200 mb equatorial easterlies over the western and central Pacific were unusually strong. Concurrently the anticyclone over the Mexican region reached maximum intensity and was displaced to the north of its normal position.

1. Introduction

The monsoon of south and southeast Asia dominates the northern hemispheric summer circulation. The upper troposphere is characterized by a quasi-stationary anticyclone anchored over Tibet with an easterly jet to its south (Ramage and Raman 1972), and mid-oceanic troughs over the Pacific and Atlantic Oceans with westerlies to their south (Krishnamurti 1971a; Sadler 1975a). The lower tropospheric circulation comprises a cyclonic centre over north India and high pressure cells over the Pacific and Atlantic Oceans. Krishnamurti (1971b) showed that for the summer of 1967, the upper anticyclone over the Himalayan region nearly coincides with the updraft portion of a thermally direct divergent circulation system possessing distinct north-south (Hadley) and east-west circulations. Holton and Colton (1972) explained the near in-phase relationship between anticyclonic vorticity and divergence over the monsoon region as being largely due to a balance between vorticity generation (through divergence) and frictional dissipation. Webster (1972) showed that the time independent summer circulations of low latitudes were satisfactorily simulated in his model with prescribed diabatic heating and orographic forcing. In addition Manabe *et al.* (1970, 1974) and Washington and Daggupaty (1975) have discussed the tropical circulation as simulated by their global general circulation models.

Despite the semipermanent nature of the summer monsoonal circulation, substantial fluctuations occur in the lower troposphere and to a lesser degree in the upper troposphere. Precipitation data over India and southeast Asia indicates a somewhat long (>10 days) period for these

*Contribution No. 76-12 of the Department of Meteorology, University of Hawaii.

changes. This variability is perhaps associated in part with sequences of time-clustered, partly overlapping monsoon lows, depressions and other transients. Fluctuations could also occur in response to barotropic and baroclinic processes within the tropics in addition to interaction with other regions. Kanamitsu *et al.* (1972) examined the barotropic energy transfers in a channel between 15°S and 15°N during the summer of 1967. Colton's (1973) one-level spectral model showed that transient waves with a wavelength range of about 6000-8000 km were the preferred modes for receiving energy through nonlinear barotropic interaction with large-scale, quasi-stationary forced waves. In Murakami's (1974) multi-level diagnostic model the steady and transient waves excited in response to specified diabatic heat sources during the summer monsoon resembled those observed.

Rather drastic changes have occasionally been observed when "break monsoon" conditions prevail over India. Murakami (1976) examined satellite cloudiness data for "active" and "break" periods which occurred during June, July and August from 1965 through 1973. He found that cloudiness fluctuations were correlated along an elongated zone covering the Indian, Malaysian, Indonesian and the western South Pacific regions. Other studies also indicate that monsoon fluctuations are an integral part of changes occurring over a fairly extensive area.

Hitherto the energetics of tropospheric fluctuations have not been studied comprehensively. Furthermore, barotropic, baroclinic and lateral coupling processes associated with temporal circulation changes remain unclear. This study attempts to shed some light on these pertinent questions. We thought that a preliminary effort had to be made to understand some of the energetics cum circulation variations as a prerequisite to the success of MONEX. To this end we have used wind data at 200 mb and 700 mb, compiled by the National Meteorological Centre, NOAA, together with satellite-derived cloudiness data, to investigate the structural and energetic features of the fluctuations in the northern summer circulation.

2. Data and computational procedures

List of symbols

λ	Longitude
θ	latitude
t	time
a	radius of earth
u,v	zonal and meridional winds
c	cloudiness amount
ζ	vorticity
$\nabla.\mathbf{V}$	divergence
ϕ	geopotential
ψ	streamfunction
χ	velocity potential
$(\overline{\ })$	zonal mean
$(\ )'$	departure from zonal mean
$<\ >$	time mean
$(\ )^*$	departure from time mean
$(\hat{\ })_n$	complex amplitude for zonal wavenumber n
K	zonal mean kinetic energy
k	eddy kinetic energy
k^*	transient eddy kinetic energy
k_n	eddy kinetic energy for zonal wavenumber n

The investigation is based on National Meteorological Center's (NMC) operational analysis of u and v data at 200 mb and 700 mb from June through August 1970. Since the analysis incorporated both commercial aircraft and ATS1/ATS3 data, we concluded that it would be accurate enough to resolve at least the large-scale aspects of circulation changes during the northern summer. Wind analyses are available for the NMC 73×23 point tropical grid, equally spaced on a mercator projection, from 48·09°S to 48·09°N. The fields of divergence as derived from the NMC wind analyses were probably somewhat smoothed, being intended for use as initial data to the NMC weather prediction models. Thus, the divergence fields associated with smaller scale disturbances may not be too realistic. However, note that *daily* maps of the upper circulation during the northern summer contain primarily long wave features.

The daily NMC wind data was used along with cloudiness data as determined by Prof. Sadler (University of Hawaii) over 2·5 degree latitude-longitude grid squares between 30°S and 30°N [The manner of data extraction is described in Sadler (1968) and Atkinson and Sadler (1970)]. Horizontal smoothing was applied to the original data over a 5° latitude by 5° longitude area to eliminate small-scale noise while retaining large-scale cloudiness perturbations of specific interest. As shown later, changes in observed divergence

(or velocity potential) agreed reasonably well with changes in cloudiness.

Daily u, v and c data were separated into zonal mean and eddy components. For example, u was expressed as :

$$u = \bar{u} + u' \tag{1}$$

Introducing the notation $< >$ to represent the seasonal mean value for the northern summer and $(\ )^*$ the departure from it:

$$u = <u> + u^* \tag{2}$$

Thus, u^* is defined as the transient component of u.

The same procedure, as described by Krishnamurti *et al.* (1971b) for the separation of horizontal winds into rotational and divergent wind components, was employed in the present study; *i.e.*, streamfunction ψ was obtained by

$$\nabla^2 \psi' = \zeta' = \frac{\partial v'}{a \cos\theta \, \partial\lambda} - \frac{\partial u' \cos\theta}{a \cos\theta \, \partial\theta} \tag{3}$$

$$\bar{\psi} = - \int \bar{u} \, a \, d\theta \tag{4}$$

In solving the Poisson equation (3) we have assumed that $\psi' = \phi'/f$ at 48.1°N and 37.1°S. The daily ϕ'-values at the boundaries were determined numerically from temperature data compiled by U.S. Navy Fleet Numerical Weather Center. When integrating equation (4), $\bar{\psi}$ was assigned to be zero at the equator.

Likewise, the velocity potential χ was obtained by

$$\nabla^2 \chi' = (\nabla \cdot \mathbf{v})' = \frac{\partial u'}{a \cos\theta \, \partial\lambda} + \frac{\partial v' \cos\theta}{a \cos\theta \, \partial\theta} \tag{3}$$

$$\bar{\chi} = \int \bar{v} \, a \, d\theta \tag{4}$$

where $\chi' = 0$ was prescribed in 48.1°N, and 37.1°S, and $\bar{\chi} = 0$ at the equator.

The dependency of eddy perturbations on longitude λ was taken to be of the form

$$\{u', v', c', \psi', \chi'\} = \sum_{n=1}^{10} \{\hat{u}, \hat{v}, \hat{c}, \hat{\psi}, \hat{\chi},\}_n e^{in\lambda} \tag{7}$$

in which we consider wave numbers up to 10 only, the amplitude for larger wavenumbers ($n>10$) being extremely small.

Zonal mean and eddy kinetic energy were computed every day for the 90-day period as follows:

$$K = \frac{1}{2} \bar{u}^2 \tag{8}$$

$$k = \frac{1}{2} \overline{(u'^2 + v'^2)} = \sum_{n=1}^{10} k_n \tag{9}$$

The transient eddy kinetic energy was computed at every NMC grid point (approximately 5 degree latitude-longitude) as follows :

$$k^* = \frac{1}{2} <u^{*2} + v^{*2}> \tag{10}$$

The Fourier representation of atmospheric motion has shed much light upon the processes of generation, dissipation, and transfer of kinetic energy in and among scales of atmospheric motions in extratropical (Saltzman 1970) and tropical (Kanamitsu *et al.* 1972) regions. Kinetic energy interactions in the Fourier domain were investigated by using equations similar to equation 49 of Saltzman (1957). However, due to limitations in NMC wind data no attempt was made in this study to estimate the vertical velocity. This, terms related to vertical motion were omitted. The transfer of kinetic energy between eddies and zonal mean flows at a latitude circle is given by

$$W\text{-}Z \sum_{n=1}^{10} (W\text{-}Z)_n = \sum_{n=1}^{10} \bar{u} \frac{\partial (\overline{\bar{u}' \bar{v}'})_n \cos^3\theta}{a \cos^2\theta \, \partial\theta} \tag{11}$$

where $(W\text{-}Z)_n$ represents the interaction of waves of wavenumber n and zonal flows.

We also computed the non-linear wave-wave interaction every day for all zonal wavenumbers 1 to 10. The interaction term for wavenumber n may be expressed as

$$(W\text{-}W)_n = -\overline{\left[u_n' \left(\frac{\partial u' u'}{a \cos\theta \, \partial\lambda} + \frac{\partial u' v' \cos^2\theta}{a \cos^2\theta \, \partial\theta} \right)_n' \right.}$$

$$\left. + \overline{v'_n \left(\frac{\partial u' v'}{a \cos\theta \, \partial\lambda} + \frac{\partial v'^2 \cos\theta}{a \cos\theta \, \partial\theta} + \frac{\tan\theta}{a} u'^2 \right)_n'} \right] \tag{12}$$

3. Seasonal mean stream-function and velocity potential

The computed 92-day (June, July and August 1970) mean stream-function and velocity potential at both 200 mb and 700 mb were used to examine the characteristics of the mean summer circulation. In Fig. 1 (top) the 200 mb $<\psi>$ field is dominated by a pronounced anticyclone centred around 25°N, 50-60°E and distinct mid-oceanic troughs over the central North Pacific and Atlantic. An easterly jet (18 m sec^{-1}) is found to the south of

the anticyclonic centre, around 5°N, 75°E, while westerlies of 14 m sec^{-1} and 8 m sec^{-1} exist to the south of the cyclonic circulations of the Pacific and Atlantic regions, near 17°N, 170°W and 22°N, 55°W, respectively. Also evident is a ridge system over the Mexico-Texas region with an anticyclonic centre near 10°N, 90°W. The southern hemisphere displays analogous features with an anticyclonic centre near 10°S, 115°E and troughs over the South Pacific and South Atlantic. Generally, easterlies dominate the tropics, while polewards of about 25°N and 10°S westerlies prevail with jet maxima embedded in them in the Caspian Sea and Australian regions. Although large-scale zonal asymmetries are found in mid latitudes, the winds are more zonal towards the equator.

Isopleths of summer mean velocity potential at 200 mb are shown in Fig. 1 (bottom), the counterpart of Fig. 1 of Krishnamurti *et al.* (1971b) with an opposite sign due to our definition of velocity potential. Large-scale similarities between the two fields are apparent. The $<\chi>$ field is dominated by an intense negative centre near 15°N, 125°E, with strong north-south and east-west circulations. Streamlines of the divergent part of the winds emanate from the active convection areas of the monsoon region and converge over the heat sink (radiational cooling) regions, between 15°N and 30°N, over the Pacific Ocean and Arabia. Outflow from the monsoon region is also carried off toward both the north and south to converge over the continental heat sink regions of North China and Australia. Thus a planetary scale, meridionally oriented, local Hadley circulation is implied with updraft over the monsoon region and downdrafts near Australia and Mongolia. The east-west circulation over the equatorial South Pacific may correspond to the so-called Walker circulation. A region of minimum χ is also encountered over the Mexican-Caribbean Sea region where monsoon type circulations and convective activity is found during the northern summer. Outflow from this area is directed to the heat sink regions of the Pacific and Atlantic Oceans.

In Fig. 1, a feature of interest is the approximate 30°-50° phase difference between the respective $<\chi>$ and $<\psi>$ centres. Holton and Colton (1972) hypothesized a predominant balance between the generation of vorticity through divergence and viscous dissipation. Their thesis was based on the observed (Krishnamurti 1971a) near in phase relationship between stream function and velocity potential over the monsoon region. It might be pointed out here that the ψ and χ fields computed from the 9-year mean wind fields of Sadler (1975a) also show an approximate 35° phase separation. This phase difference could, conceivably, vary from year to year.

The 700 mb $<\psi>$ field, Fig. 2 (top) shows a prominent cyclonic low centred over India; westerlies to its south extend to 5°S. A weak monsoon trough lies northwest-southeast across the Bay of Bengal, southeast Asia and Borneo regions. The trough extends east-west over India and northeast-southwest over the Arabian Sea to the Somalia region (*see* also, Ramage and Raman 1972). Along about 30°N strong anticyclonic circulations dominate the surface high pressure regions of the central Pacific and Atlantic, with trade winds over equatorial latitudes. The southern hemisphere is characterized by an east-west near-equatorial trough lying along about 5°S over the south Indian Ocean with westerlies to the north and easterlies to the south. A pronounced ridge system extends around the globe along 15°S with maximum centres over the South Pacific and Atlantic regions. A comparison of Fig. 1 (top) and Fig. 2 (top) reveals cyclonic (anticyclonic) cells in the lower troposphere lying beneath anticyclonic (cyclonic) circulations in the upper troposphere.

In Fig. 2 (bottom), depicting the 700 mb $<\chi>$ field, χ-maximum centres with convergent inflow lie beneath 200 mb χ-minimum centres of divergent outflow, and *vice versa*. This is consistent with the implication of mid-tropospheric updraft and downdraft in conjuction with centres of low and high velocity potential in the upper troposphere.

Fig. 3 (top) depicts the mean 200 mb divergence field. The large-scale features comprise areas of divergence over India, southeast Asia, Mexico and equatorial South America, and areas of convergence over the North and South Pacific and Atlantic, the equatorial Central Pacific dry zone and the desert regions of Arabia and Australia. A band of large divergence extends from the Indian-southeast Asia region, across the equator and New Guinea to the western South Pacific. Also, zones of divergence lie along about 7°N over the central and eastern Pacific. Over the Asiatic monsoon region, the divergence maximum over the

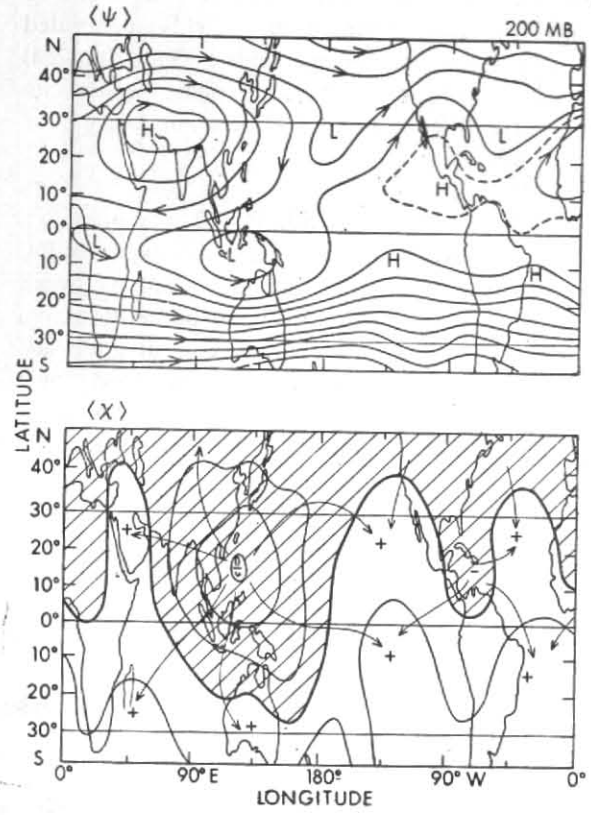

Fig. 1 (Top) : Mean 200 mb stream function, $<\psi>$, in units of 10^6 m^2 sec^{-1}. Interval 10 units. Arrows indicate the direction of the nondivergent winds.

(Bottom) : Mean 200 mb velocity potential, $<\chi>$, in units of 10^6 m^2 sec^{-1}. Interval 2 units. Arrows represent the direction of divergent winds. Both $<\psi>$ and $<\chi>$ were computed from Eqns. (3) to (6) with the zonal mean component included.

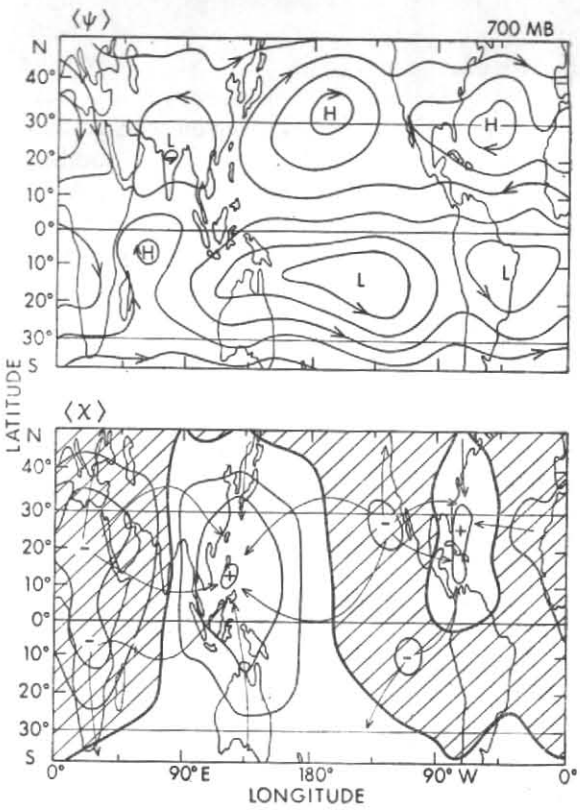

Fig. 2 As in Fig. 1, but for 700 mb. Isopleth interval is 5×10^6 m^2 sec^{-1} for $<\psi>$ and 1×10^6 m^2 sec^{-1} for $<\chi>$

southeast Asia-Philippines area seems to dominate the maxima near India (15°N, 85°E) and Tibet (32°N, 95°E). Divergence computed from Sadler (1975a), representing 9-year mean conditions, exhibits similar features. However, for the summer of 1967 Krishnamurti (1971b) shows a dominant divergence maximum over the Tibet-China region along about 30°N-35°N. During any one particular year, the dominant centre could, conceivably, lie either over southeast Asia or Tibet.

In Fig. 3 (bottom), zones of 700 mb convergence (divergence) lie beneath those of 200 mb divergence (convergence) as expected. However, over some areas such as the Himalayas 700 mb divergence, as determined from NMC data, may be questionable.

In Fig. 4 (top) India and southeast Asia are cloudy, while a relatively cloudy extension crosses the equator and New Guinea, to the western South Pacific off the east coast of Australia. This band coincides with large 200 mb divergence. The near-equatorial large cloudiness zone circles the globe along about 7°N, approximately in the same location as upper (lower) tropospheric divergence (convergence). The central Pacific dry zone has little cloud (Cloudy regions off the west coast of the Americas are composed mainly of

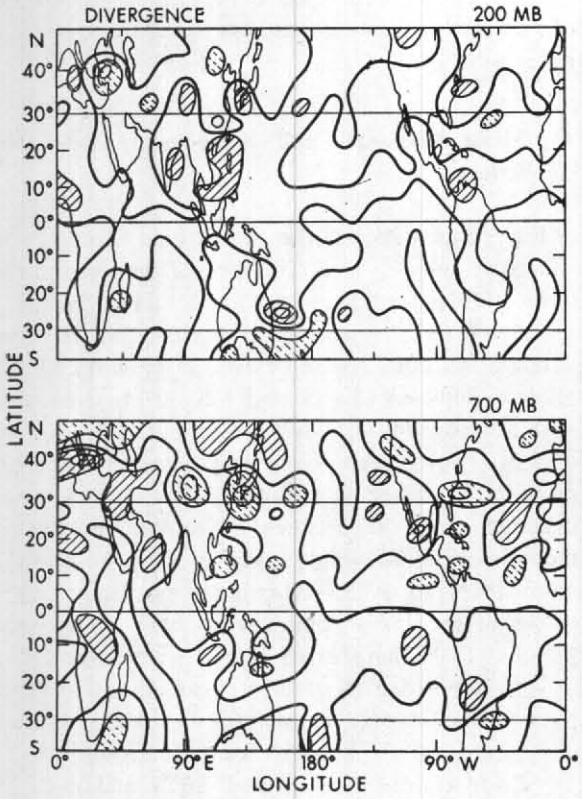

Fig. 3. Mean divergence.

(Top): 200 mb. Interval 2×10^{-6} sec^{-1}. Regions of divergence greater than 2×10^{-6} sec^{-1} are hatched, less than -2×10^{-6} sec^{-1} are dashed hatched.

(Bottom): 700 mb. Interval 1×10^{-6} sec^{-1}. Regions of divergence greater than 1×10^{-6} sec^{-1} are hatched, less than -1×10^{-6} sec^{-1} are dashed hatched.

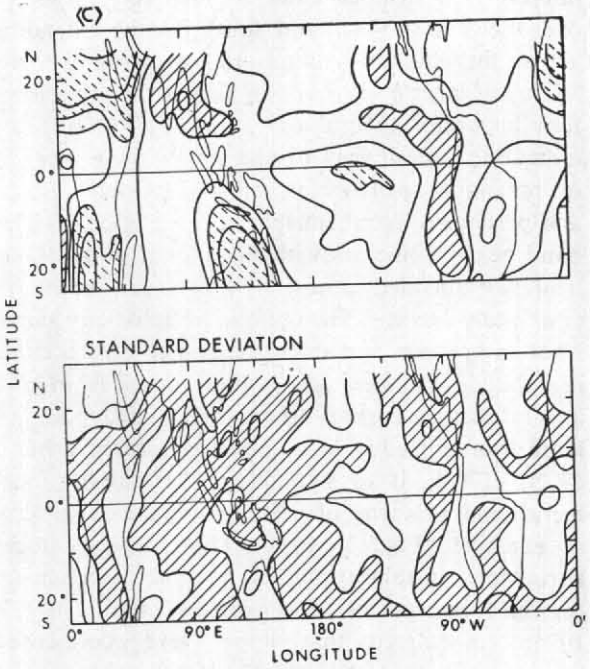

Fig. 4 (Top): Mean cloudiness amount in oktas. Regions of $<c>$ greater than 5 okta are hatched, $<c>$ less than 3 okta are dashed hatched.

(Bottom): Mean cloudiness standard deviation. Interval 0·5 okta. Regions of standard deviation exceeding 1 okta are shaded.

stratus decks and are not actively convective). In general, fair agreement exists between the fields of season mean cloudiness and divergence†.

Fig. 4 (bottom) depicts the standard deviation of of season mean cloudiness, a measure of cloudiness variability associated with disturbances in the tropospheric circulation. Generally, in cloudy regions the standard deviation is large and *vice versa*. Some areas, where large standard deviation is accompanied by low mean cloudiness, probably experience dry weather most of the time, occasionally interrupted by brief severe wet periods.

Fig. 5 (top) shows the 200 mb distribution of transient eddy kinetic energy k^* computed from equation (10)††. k^* is notably small between about 5°S and 20°N, in marked contrast to large k^* values poleward of about 25°N and 10°S. Maxima (>200 m^2 sec^{-2}) are encountered around Japan, Australia and the western South Pacific where the upper tropospheric westerlies frequently change in intensity and location. Transient eddy kinetic energy over the monsoon region is conspicuously small (<50 m^2 sec^{-2}) owing to the dominance of quasi-stationary circulation components, with the tropical easterly jet being fairly steady. Although

†Correspondence between cloudiness (an independent variable) and divergence, perhaps affirms the validity of NMC data.

††Transient eddy kinetic energy obtained from NMC data was compared with that computed from station data at Calcutta, Gan, Singapore, Tateno, Majuro and Lihue with excellent agreement. Perhaps this justifies the use of NMC operational data in as far as the examination of large-scale circulation changes during the northern summer is concerned.

circulation fluctuations over the monsoon region are small compared to mid-latitudes, they are not necessarily negligible in the context of tropical motions, as will be shown later. Of particular interest is a distinct band of relatively large k^* over the central North and South Pacific, extending across the equator around 150°W [Interestingly, a band of large k^* is found in almost the same location in winter (Murakami *et al.* 1976), possibly indicating that all year around the Pacific is a region of maximum penetration of mid-latitude effects and perhaps of interhemispheric interaction]. This band nearly coincides with the axes of mid-oceanic troughs embedded in westerly flows over the North and South Pacific. The oceanic troughs vary somewhat in position and intensity, sometimes facilitating the development of cyclonic vortices in and around them. Perhaps, then, the isolated pool of large transient eddy kinetic energy located around 19°N, 170°E, is of significance. Here, the local meridional gradient of 200 mb absolute vorticity is negative (Fig. 1, top). This suggests local barotropic instability as a possible mechanism for the formation of these vortices. Sadler (1967, 1975b) postulated that upper level cold-cored lows develop in relatively cloud free regions and occasionally intensify further when they trigger off cumulus convection through some unknown vertical coupling mechanism. However, other areas of negative meridional gradient of absolute vorticity near, for example, the easterly jet over the equatorial Indian Ocean, do not seem to be associated with large k^*.

At 700 mb (Fig. 5, bottom) over the tropical Central Pacific, where the trade wind easterlies are persistent and steady, transient eddy kinetic energy is very small. In contrast to other tropical areas, transient eddies are evidently most active (large k^*) over the Indian, North and South Indian Ocean, and Australian regions : (1) Over the Bay of Bengal large k^* is undoubtedly associated with monsoon lows and depressions developing over that region and moving northwestwards over India; (2) over Arabia-Somalia large k^* is probably related to velocity fluctuations in the northerly-northwesterly flows there; (3) over the equatorial Indian Ocean large k^* probably reflects disturbance activity in the vicinity of the southern hemisphere near-equatorial trough. Yet another zone of large k^* extends from mid-latitudes, across Japan to the equatorial-Borneo region. Perhaps, this represents a possible route through which the low-level monsoon circulation interacts with mid-latitude systems. Overall, the distributions of 700 mb k^* and cloudiness standard deviation agree well.

4. Mean wave-wave and wave-zonal flow interaction

Fig. 6 (top) shows the meridional distribution of $<\bar{u}>$ and $<\bar{v}>$ at 200 mb. The zonal mean $<\bar{u}>$ flow is westerly to the north of 19·6°N with a maximum (~22 m sec^{-1}) at about 41°N. In intervening latitudes there exists large anticyclonic shear. Between 19·6°N and 5°S, $<\bar{u}>$ is easterly with a maximum of about 7 in sec^{-1} at 5°N. South of 5°S, $<\bar{u}>$ reverts to westerly flows with a maximum (~34 m sec^{-1}) around 33°S and large anticyclonic shear in between. Negative (northerly) mean meridional wind $<\bar{v}>$ extends southward from 19°N to 37°S. Maximum northerly $<\bar{v}>$ (—0·8 m sec^{-1}) is found at about 3°N. Between 3°N and 15°N there exists large $<\bar{v}>$ divergence. $<\bar{v}>$ is positive (southerly) from about 19°N to 26°N. The Hadley circulation is, thus, implied with its updraft branch located around 10°N-15°N and downdrafts around 26°N and over an extensive region in the southern hemisphere (N-S overturnings over the monsoon region contribute most to this mean Hadley cell). The northern hemisphere Hadley is considerably weaker than its southern hemisphere counterpart. These findings conform to the observations of Oort and Rasmusson (1971). Above 26°N, $<\bar{v}>$ is northerly reaching 0·25 m sec^{-1} around 41°N. Flows in this region correspond to the indirect mid-latitude Ferrel cell of the northern summer hemisphere.

Fig. 6 (bottom) shows the near-equatorial cloudy zone near 7°N. Also, $<\bar{c}>$ maximum appears to be associated with a region of large $<\bar{v}>$ divergence at 200 mb. $<\bar{c}>$ drops off sharply to the north of about 10°N and is small above about 26°N, where the descending leg of the northern hemisphere Hadley is found. South of the equator, the small gradient of $<\bar{c}>$ is associated with uniform and small $<\bar{v}>$ convergence.

The computed momentum transports due to standing eddies, $\overline{<u>'<v>'}$, and transient eddies, $\overline{<u'^*v'^*>}$ at 200 mb are also shown in Fig. 6 (bottom). In general, momentum transport due to transient eddies is positive (northward transport) over the northern hemisphere and

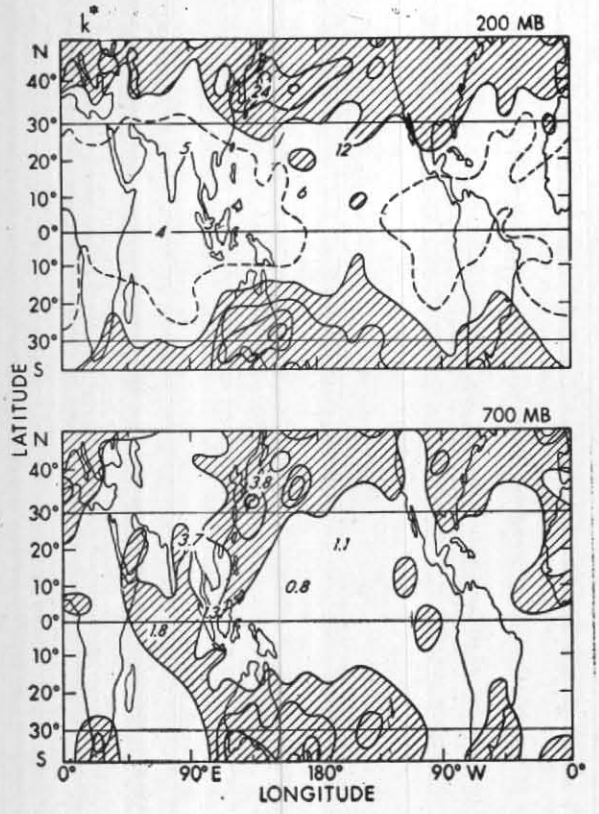

Fig. 5 (Top) : Transient eddy kinetic energy at 200 mb computed from Eq. (10) in units of 10 m^2 sec^{-2}. Interval 10 units. Regions of $k^* > 10$ units are shaded.

(Bottom) : k^* at 700 mb in units of 10 m^2 sec^{-2}. Interval 2 units. Regions of $k^* \geq 2$ units are shaded. Transient eddy kinetic energy computed using station data at Calcutta, Gan, Singapore, Tateno, Majuro and Lihue are shown in italic numerals.

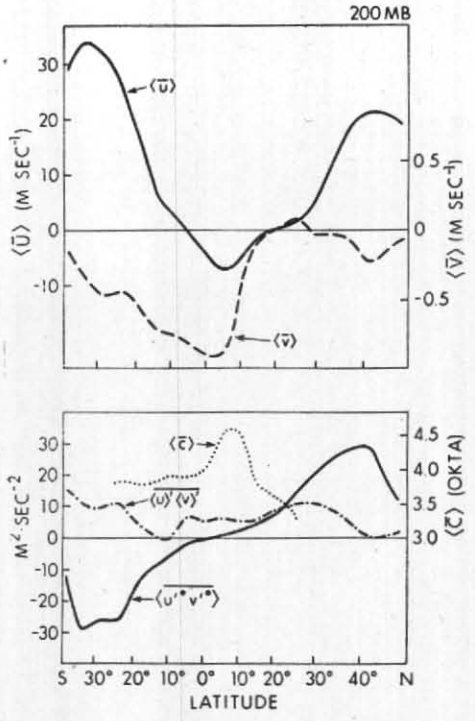

Fig. 6. 200 mb meridional distribution of mean $\langle\bar{u}\rangle$, $\langle\bar{v}\rangle$, $\langle\bar{c}\rangle$ and of momentum transport due to standing eddies, $\overline{\langle u\rangle' \langle v\rangle'}$, and transient eddies $\overline{\langle u'^* v'^*\rangle}$

negative (southward) over the southern hemisphere. Cross-equatorial momentum flux appears to be largely due to standing eddies and amounts to about $+5$ m^2 sec^{-2}. The northward momentum transport due to transient (standing) eddies amount to about 30 (10) m^2 sec^{-2} at 40 (28) N. These values are in fair agreement with measurements by Oort and Rasmusson (1971). Between about 20°N and 35°N there is a large horizontal divergence of net momentum flux. Though considerably weaker, flux divergence extends into equatorial regions as well. This results in a westerly deceleration (or easterly acceleration) of the zonal mean winds there. North of about 35°N net momentum flux convergence is encountered.

The wave-zonal mean flow interaction depends sensitively on the sign and magnitude of the zonal mean flow and momentum flux divergence. Table 1 (top) shows the latitude-wavenumber dependency of the wave-zonal mean flow interaction terms computed at 200 mb for wavenumbers 1 to 10. The sum of contributions due to each wavenumber, $(W\text{-}Z)_n$, is equal to the net $(W\text{-}Z)$, as defined in Eq. (11). Poleward of about 41°N, $(W\text{-}Z)_n$ is generally negative, a negative sign indicating the transfer of kinetic energy from wave of wavenumber n to zonal mean flows. Over tropical latitudes from about 5°S to 19·6°N, $(W\text{-}Z)_n$ is comparatively small and mostly negative, easterly $\bar{u}$ being associated with weak momentum flux divergence. Kanamitsu *et al.* (1971) computed the wave-zonal mean interaction term at 200 mb over a tropical belt from 15°S to 15°N for the northern summer of 1967. They found large transfers of kinetic energy from waves of wavenumber 1 to zonal mean flows. In

TABLE 1

Energy exchange (10^{-6} m^2 sec^{-3}) between waves and zonal mean flows (top) and between waves (bottom) at 200 mb, averaged for a 92-day period covering June 1970 through August 1970

	LATITUDES																		
N	−37·1	−33·0	−28·7	−24·2	−19·6	−14·8	−10·0	−5·0	0·0	5·0	10·0	14·8	19·6	24·2	28·7	33·0	37·1	41·0	44·6	48·1
N=1	−138	−20	95	−148	−150	−29	14	−4	22	0	−2	6	2	−6	−59	−138	−132	−5	183	228
N=2	85	18	−68	−81	−45	−5	10	−1	1	2	4	−8	−6	−4	11	31	38	−32	−161	−201
N=3	−200	−113	−13	−12	−2	6	2	−2	−15	−5	0	1	2	7	22	0	−108	−127	−34	8
N=4	−97	−71	−4	44	42	16	6	−2	−1	2	2	−3	−4	3	11	−1	−15	−31	−71	−63
N=5	−117	−107	−59	80	91	18	6	0	−4	−3	2	0	0	6	5	22	55	−5	−55	−47
N=6	−313	−200	11	118	68	14	7	−1	−3	−2	−2	0	1	4	8	5	−45	−70	−48	−37
N=7	−250	−125	24	56	50	12	1	0	0	−2	−2	0	2	3	7	5	−10	−27	−104	−155
N=8	−143	−48	19	16	28	7	2	0	4	2	−2	0	1	4	11	−6	−11	13	−37	−70
N=9	−125	−58	7	15	22	8	1	1	0	−2	−3	−1	0	2	1	−14	−27	−42	−52	−54
N=10	−52	−23	3	10	11	3	0	0	−2	−2	−1	0	1	0	0	9	6	−34	−59	−47
N=1	−150	−40	126	15	41	46	27	−18	−2	−1	−14	26	28	−16	−29	−61	−104	−102	−69	−11
N=2	−129	−59	51	31	13	9	0	−15	−6	−14	−26	−29	−38	−38	−45	−28	11	−4	0	54
N=3	−61	−91	2	39	3	6	2	18	2	−16	−13	−3	0	18	33	21	0	−39	−70	−80
N=4	−71	−69	−112	−75	−55	−12	19	8	6	−2	−1	−8	−10	11	17	−8	3	40	28	25
N=5	−60	−66	−45	−54	−23	1	−10	−5	−1	−1	−5	−13	−6	3	12	31	−7	−94	−82	−43
N=6	−19	−74	−42	9	18	12	8	0	0	2	0	−1	0	12	12	18	42	68	55	12
N=7	−30	−4	30	6	17	8	10	8	0	2	−1	−1	−5	−13	−13	23	27	−53	−53	−30
N=8	27	27	−12	−5	4	5	−1	−3	0	−4	−5	−2	0	−3	6	28	15	−9	−39	−39
N=9	−40	7	32	36	7	3	0	−1	−1	−3	−4	0	7	0	11	8	9	13	−15	−20
N=10	21	36	37	26	15	2	0	1	0	1	−1	0	9	5	3	10	20	6	−12	−19

Table 1 (top), $(W\text{-}Z)_1$ is large and negative below 14.8°S, westerly $\bar{u}$ being associated with momentum flux convergence due to $n=1$ wave. 15°S being embedded in zonal mean westerly flows cannot, perhaps, be considered tropical in character†. Thus, caution must be exercised in order that the computation of energetics in the Fourier domain is not applied to too large a latitudinal span, lest entirely different circulation regimes be compounded together. In the present study, we have chosen three different latitudinal belts as follows :

(1) *Tropical belt* (*5·0°S-19·6°N*) : Easterly $\bar{u}$, a region enveloping that of maximum northerly $<\bar{v}>$ and $<\bar{v}>$ divergence, maximum $<\bar{c}>$, the the rising branch of the mean meridional Hadley cell and small transient eddy kinetic energy k^*.

(2) *Subtropical belt* (*24·2°N-37·1°N*): Westerly $\bar{u}$ with large anticyclonic shear, a region of negative meridional gradient of $<\bar{v}>$ and the descending branch of the northern hemisphere Hadley cell, minimum $<\bar{c}>$, large net momentum flux divergence and large k^* at 200 mb.

(3) *Mid-latitude belt* (*41·0°N-48·1 N*) : Westerly $\bar{u}$ maximum with cyclonic shear, a region with northerly $<\bar{v}>$ of the thermally indirect Ferrel cell, net momentum flux convergence and large k^* at 200 mb.

Fig. 7 depicts the wavenumber dependency of eddy kinetic energy k_n, wave-zonal mean flow interaction $(W\text{-}Z)_n$ and wave-wave interaction $(W\text{-}W)_n$, averaged over each latitudinal region for $n=1$ to 10.

In the mid-latitude belt, most waves lose energy to zonal mean flows through wave-zonal flow interaction. Waves of wavenumber 2 and around 6 and 7 contribute most. Saltzman (1970) speculated that waves of wavenumber 2 and 3 were maintained by energy sources originating from land-ocean contrasts. $n=5$, 7, 8, etc lose energy, through non-linear barotropic interactions, to both zonal mean flows and to other waves. Presumably, these waves are maintained by baroclinic instability processes. The above results are in fair agreement with those determined by Saltzman and Teweles (1964) for the 500 mb level, for a 10-year period.

Over the *subtropical belt* ultralong waves (1 and 2) and other waves (3 and above) are clearly separated, with $n=1$ and 2 wave losing energy to higher wave numbers *via* wave-wave barotropic exchange. Wavenumber 1 also loses energy to zonal mean flows. $n=1$ and 2 waves may derive their energy from such subtropical heat sources as those near and around the Tibetan massif (mid-tropospheric sensible and latent heat source) and from land-sea contrast. A secondary maximum in wave-wave energy transfers is noted at $n=8$. Daily NMC maps indicate that small vortices, apparently unconnected to convection, frequently, develop in the oceanic trough over the central North Pacific. Perhaps barotropic non-linear processes are responsible for the development of these vortices with a wavenumber of approximately 8.

As compared to the subtropical and mid-latitude belts, the energy exchanges over the *tropical belt* are marked by small $(W\text{-}Z)_n$ interaction. Although these exchanges are small, they could be significant in relation to the observed low values of eddy kinetic energy (k_n) in this region. $(W\text{-}W)_n$ interactions are also small but somewhat larger than $(W\text{-}Z)_n$ interactions. Wave number 2, in particular, loses substantial amounts of kinetic energy to other waves. Most probably $n=2$ wave is maintained through tropical baroclinic processes with E-W overturnings (associated with the active tropical convection centres) converting eddy available potential energy to eddy kinetic energy. There was no evidence to suggest that in the tropics waves of approximately wavenumber 8 are the preferred modes of receiving energy from other waves. Note also that the tropics are characterised by an overwhelming dominance in eddy kinetic energy of wavenumber 1 (k_1).

5. Temporal variations in kinetic energy

Figures presented in this section refer to total eddy (k) and zonal mean (K) kinetic energy computed daily at 200 mb and 700 mb for the entire 92-day period, over selected latitudinal belts. The time series of daily k values were found to contain somewhat substantial day to day variations. A 3-day, weighted (0·25, 0·5, 0·25) running mean was, therefore, applied to filter out short period fluctuations not of specific interest to this study.

Fig. 8 (top) depicts changes in k at 200 mb averaged over the tropical belt. A cursory glance

†The belt of zonal mean easterly flows shifts annually. During the winter of 1970, zonal mean easterlies were found between about 14·8°S and 5°N (Murakami *et al.* 1976) but between 5°S to 19·6° N in summer 1970.

reveals somewhat systematic fluctuations of a 10-15 day period. Krishnamurti *et al.* (1976) detected a dominant spectral peak around 13 days for many elements of the monsoon system. Murakami and Frydrych (1974) showed that the upper tropospheric response over the monsoon region was largest to prescribed diabatic heat sources of a 12-16 day period range. Computations of the local area contribution to k changes at 200 mb (not shown) revealed that fluctuations over the monsoon tropics (35°E-125°E) and that over the Pacific (145°E-125°W) and over the whole tropical belt (k) were very nearly in phase. Over the Pacific changes were somewhat larger than over the monsoon region — consistent with the finding that k^* is larger over the former area.

Fig. 8 (bottom) shows the corresponding k changes averaged over the 700 mb tropical belt. Primary maxima exist around days 12-16, 38-39 and 78-80. In addition to these long-period variations, much shorter period (~5 day) fluctuations also occur. These may be attributed to the passage of weak disturbances, monsoon lows, etc, at the 700 mb level. The eddy kinetic energy changes at 700 mb and 200 mb are not obviously related. However, from about day 41 to 55, k at both levels decreases in synchrony to reach minimum values around day 50-54. Because this period had unique characteristics (compared to any other period), it has been singled out for a more detailed examination later. It is noteworthy that the India Meteorological Department reported "break monsoon" conditions prevailing over India from 12 to 25 July 1970.

In Fig. 9 (top), changes in eddy and zonal mean kinetic energy, over the 200 mb tropical belt, are negatively correlated during most of the 92 days. Around day 42, changes in eddy and zonal mean kinetic energy are large, of the same order, and of opposite sign. However, computations of changes in the (W-Z) term failed to corroborate a transfer of energy from eddies to zonal mean flows. At this juncture, it is worth pointing out that northerly $\bar{v}$, averaged over the 200 mb tropical belt, strengthened from −0·3 m sec^{-1} at day 40 to −1·0 m sec^{-1} on day 44 (season mean value is approximately −0·5 m sec^{-1}). This $\bar{v}$ change appears have led to an increase in easterly $\bar{u}$ during that period (200 mb zonal mean easterlies approach maximum speeds at this time). This, of course, is reflected in increased K over the tropical belt.

In contrast, kinetic energy changes *prior to* day 40 showed some correspondence with changes in the (W-Z) interaction term. Positive peaks in (W-Z) interaction of about 2×10^{-5} m^2 sec^{-3} above normal were observed around days 2-3, 15-16 and 27-28. The amplitude of k changes was of the order of 20 m^2 sec^{-2}, while that of K amounted to about 7 m^2 sec^{-2}, the corresponding rate of change in k (K) being approximately $5\,(2)\times10^{-5}$ m^2 sec^{-3}. Perhaps, then, wave zonal mean interaction can account for about one third of the total change in eddy kinetic energy. In short, even prior to day 40, barotropic transfers between eddies and zonal mean flows do not completely account for the changes in eddy kinetic energy.

In the present study, we have not directly evaluated energy generation due to baroclinc processes related to the correlation between vertical motions and temperature perturbations. Instead we computed $\overline{c'^2}$ everyday over a region from 5°S to 20°N; Fig. 9 (bottom). Using a set of linearized primitive equations with heat sources prescribed as external forcing, Holton (1971) showed that upper tropospheric temperatures were high just above prescribed heating and strong upward motion associated with easterly waves of zonal wavelength ~4000 m. Murakami (1974) also demonstrated that high temperatures nearly coincided with regions of ascending motion and heat sources (assumed propotional to cloudiness) in large scale monsoon flows. Conceivably, then, $\overline{c'^2}$ may be an approximate measure of baroclinic processes in the tropics. In Fig. 9 (bottom) $\overline{c'^2}$ maxima around days 12-16, 38-42 and 78-82 nearly coincide with k maxima at 700 mb.

Interestingly, between day 50 and 54, $\overline{c'^2}$ and k at 200 mb and 700 mb were all well below their season mean values, while 200 mb K was at its maximum.

Next we examine the possibility of mid-latitude effects on eddy kinetic energy pulsations in the tropical belt. Fig. 10 (top) clearly shows a long period (~20 days) variation in 200 mb mid-latitude eddy kinetic energy [Webster and Kellar (1975) observed that the eddy kinetic energy of the upper troposphere between about 30°S and 60°S derived from EOLE constant density balloon data, possessed a strong 18-23 day fluctuation]. Of interest are the maxima in mid-latitude k around days 4-5 and 29-30 which precede peaks in tropical k (*see* Fig. 8, top) around days 5-7 and 32-33.

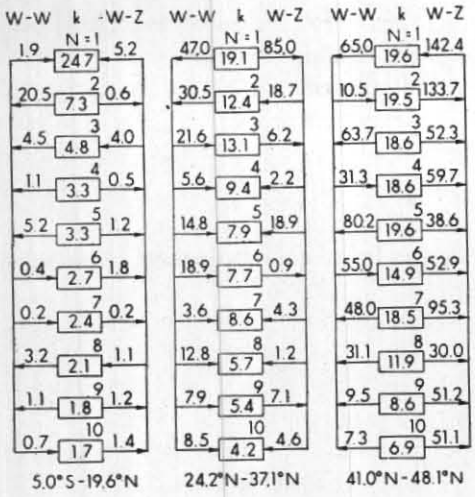

Fig. 7. 200 mb mean eddy kinetic energy, k_n, in units of 1 m^2 sec^{-2}, energy exchange between waves, $(W\text{-}W)_n$, and between waves and zonal mean flows, $(W\text{-}Z)_n$, in units of 10^{-6} m^2 sec^{-3}, for zonal wavenumbers $n = 1$ to 10, averaged over the mid-latitude belt (41·0°N-48·1°N), subtropical belt (24·2°N-37·1°N) and tropical belt (5·0°S-19·6°N), respectively

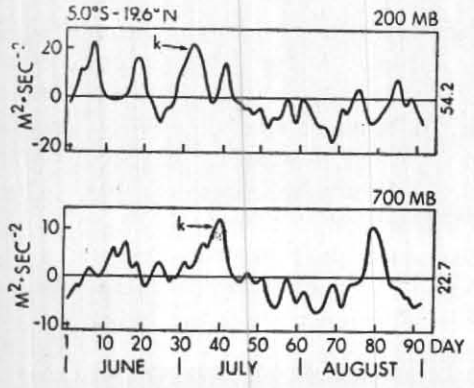

Fig. 8. Time series of 3-day running mean eddy kinetic energy k at 200 mb (top) and 700 mb (bottom), averaged over a tropical belt between 5°S and 19·6°N. The curves are drawn with the summer mean values used as zero reference; *i.e.*, $<k>$ at 200 mb = 54·2 m^2 sec^{-2} and $<k>$ at 700 mb = 22·7 m^2 sec^{-2}

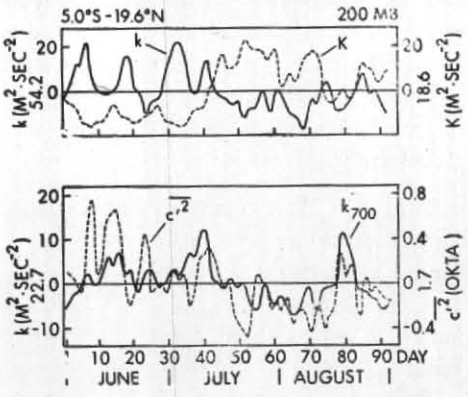

Fig. 9 (Top) : Time series of 3-day running mean eddy kinetic energy (solid) and zonal mean kinetic energy (dashed), averaged over the 200 mb tropical belt from 5°S to 19·6°N. Season mean values used as zero reference for the curves are : $<k>$ = 54·2 m^2 sec^{-2} and $<k>$ = 18·6 m^2 sec^{-2}.

(Bottom) : Time series of 3-day running mean k at 700 mb (solid) and $\overline{c'^2}$ (dashed). Season mean values used as zero reference are : $<k>$ = 22.7 m^2 sec^{-2} and $<\overline{c'^2}>$ = 1·7 okta²

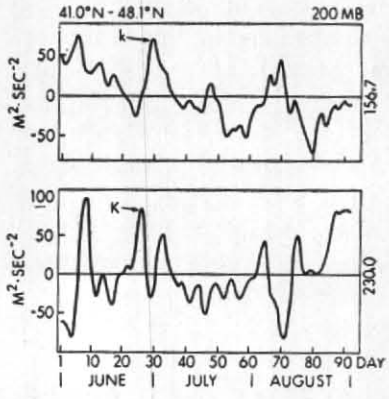

Fig. 10. Time series of 3-day running mean eddy kinetic energy k (top) and zonal mean kinetic energy k (bottom), at 200 mb, averaged over the mid-latitude belt from 41·0°N to 48·1°N. Season mean values used as zero reference for the curves are : $<k>$ = 156·7 m^2 sec^{-2} and $<k>$ = 230·0 m^2 sec^{-2}

Whether this means that mid-latitude effects propagate into tropical latitudes to cause fluctuations in the eddy kinetic energy there, is not of course clear, even though conceivable. Significantly, mid-latitude k and tropical k are both well below normal between day 50-54.

Fluctuations in 200 mb zonal mean kinetic energy (K) (Fig. 10, bottom) are not as systematic as in k. Sometimes, as around day 70, for example, a minimum in K appears to be associated with a maximum in eddy kinetic energy. The (W-Z) interaction term was well above normal around day 66-67. Perhaps, barotropic exchange processes were significant during this period. In contrast, around days 5-7 and 32-33, when k reached maximum values, the (W-Z) term was near or even below normal. Changes around these days are probably associated with baroclinic processes in the midlatitude region. Zonal mean kinetic energy remained below season mean between day 37 and 60. The mid-latitude vertical wind shear, as defined by the difference between zonal mean $\bar{u}$ at 200 mb and 700 mb, closely follows the time variation in K. Between day 50 and 54, vertical shear was at an all-season low. Thus, in the mid-latitudes, baroclinic activity was perhaps at a minimum through the anomalous period day 50-54, compatible with the simultaneous occurrence of extremely small values of 200 mb eddy kinetic energy (Fig. 10, top).

Fig. 11 shows a longitude-time section of 200 mb zonal winds along the equator. The equatorial easterlies dominating the monsoon region with a maximum centred around 90°E are relatively steady. In comparison, changes are somewhat larger over the equatorial Pacific with winds shifting from easterly to westerly flows, probably in association with changes in the intensity and location of the oceanic troughs. Prior to day 50, westerlies generally prevailed over the equatorial Pacific. After day 50 easterlies occurred considerably more frequently. Over this region climatology confirms that westerlies are more evident during early summer while easterlies dominate later in the season. Of particular interest is the occurrence of extraordinarily strong easterlies over the equatorial western and central Pacific, between about day 50 and 54. This possibly determined the intensification of zonal mean easterly $\bar{u}$ and thus K (Fig. 9, top) over the tropical belt.

In summary, abnormal changes began around day 40 with 200 mb tropical and mid-latitude eddy kinetic energy decreasing to below season mean values. Simultaneously, 700 mb k and tropical baroclinic activity as measured by $\bar{c}^2$ also decreased; all reached minimum values around day 50-54. During the same period, 200 mb tropical zonal mean kinetic energy reached a maximum accompanied by anomalously strong easterlies over the western and central equatorial Pacific.

6. Changes in stream function and velocity potential

Fig. 12 (top) shows semipermanent features dominating the time series of 200 mb ψ along 21·9°N. A zone of high stream function (anticyclonic circulation), centred around 55°E, overlies the monsoon regions of India and southeast Asia. In contrast, the central Pacific and Atlantic regions are characterized by low stream function (cyclonic). Anticyclonic circulations between 90°W and 120°W intensified around day 50 or so, indicating that monsoonal flows over the Mexican locale developed late in summer. Long-term, 9 year, monthly mean analyses of Sadler (1975a) also showed this anticyclonic cell intensifying and shifting northwards from June to July.

Fig. 12 (bottom) presents the counterpart of Fig. 12 (top) for the field of 200 mb velocity potential along the latitude 17·2°N. Clearly perceptible is a band of minimum χ (updraft) located around 125°E. The χ field is generally positive over the Arabian and Pacific regions of upper inflow and sinking motion. The Mexico area around 90°W is the site of a secondary zone of χ minimum.

Major singularities occurred around day 50-54 (Fig. 12, top). A pool of high stream function (ridging) appeared at about 145°E over the western Pacific. ψ values around 180°E (mid-Pacific trough) become positive as opposed to normally negative. Unusually large positive ψ valves prevailed around 125°W. Anomalous features are also noticeable in the time series of χ in Fig. 12 (bottom). Around 125°E, large and negative χ values were replaced by positive values.

The next section scrutinizes the circulation features characterizing the abnormal period between day 50 and 54.

7. Circulation during the abnormal period 20-24 July

Fig. 13 (top) presents the horizontal field of 200 mb stream function averaged over the period 20-24

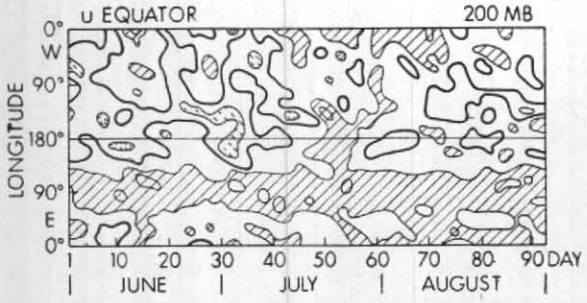

Fig. 11. Time-longitude section along the equator of 3-day running mean u-component winds, at 200 mb. Interval 10 m sec^{-1}. Regions of $u<-10$ m sec^{-1} are hatched, $u>10$ m sec^{-1} are dashed hatched.

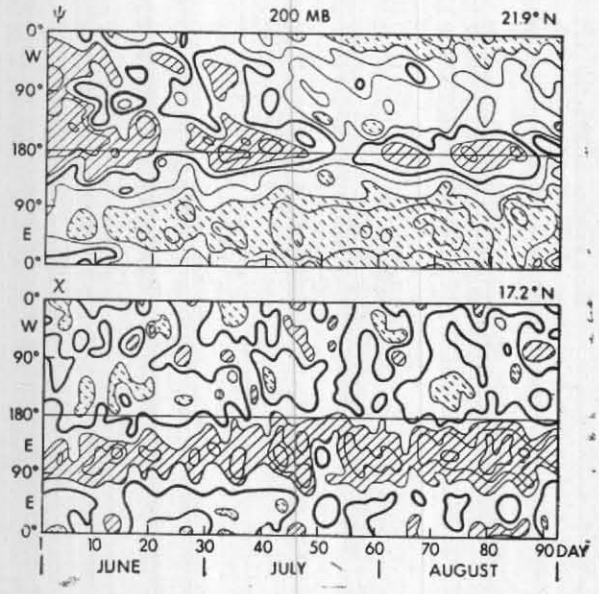

Fig. 12 (Top): Time-longitude section of 3-day running mean stream function ψ along 21·9°N in units of 10^6 m^2 sec^{-1}. Interval 10 units. Regions of $\psi <-10$ units are hatched, $\psi >$ 10 units are dashed hatched.

(Bottom): Isopleths of 3-day running mean velocity potential χ along 17·2°N in units of 10^6 m^2 sec^{-1}. Interval 3 units. Regions of $\chi <-3$ units are hatched, $\chi>3$ units are dashed hatched.

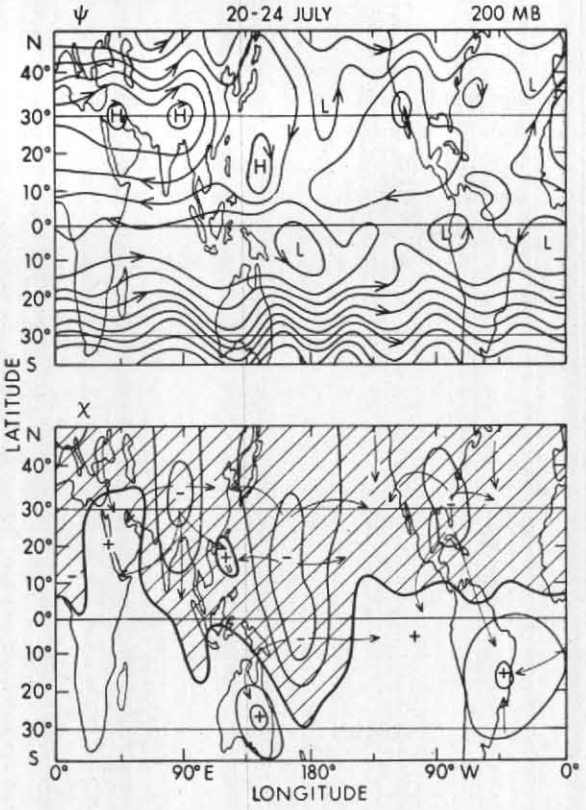

Fig. 13. As in Fig. 1, but for the period 20-24 July

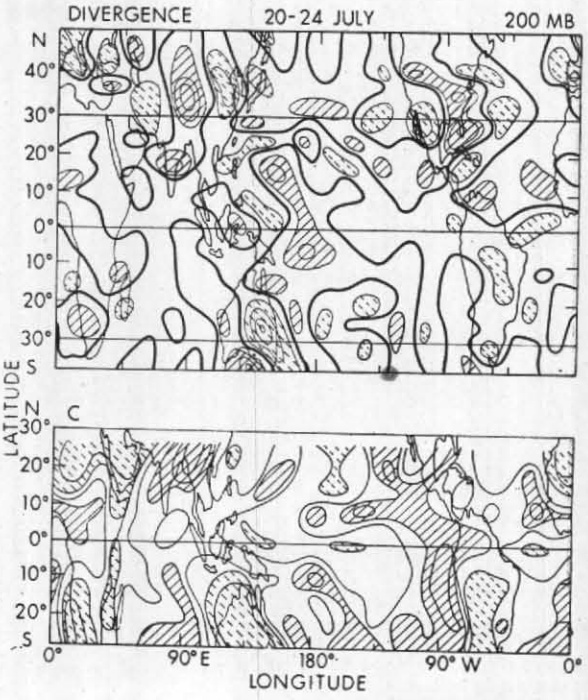

Fig. 14 (Top) : As in Fig. 3 (top), but for the period 20-24 July.
(Bottom) : As in Fig. 4 (top), but for the period 20-24 July.

July (50-54 day). This is to be compared with Fig. 1 (top) depicting season mean conditions. Marked differences are observed over the monsoon and western Pacific regions of both northern and southern hemispheres. The anticyclonic circulation over the Himalayan region bifurcated into two cells due to a trough in the mid-latitude westerlies penetrating into the subtropics along about 65°E. Extensive ridging (troughing) along about 135°E-150°E (110°E-120°E) extended over all northern latitudes. A strong anticyclonic cell (~15°N, 145°E) developed in the zone of abnormal upper tropospheric ridging. Over the western South Pacific a strong anticyclonic circulation was centred around 10°S, 175°E, accompanied by a decrease in anticyclonic flows over the North Australia-Indonesia region around 10°S, 115°E (*see* Fig. 1, top). The sudden intensification of equatorial easterlies in the western and central Pacific appears to be largely in response to the development of these anticyclonic cells straddling the equator.

Changes also occurred over the eastern Pacific-Mexico area; namely, a strengthening and northward displacement (15°N to 30°N) of the anticyclonic circulation over that area, along with the extension of a somewhat better defined ridge system into the tropical central Pacific. The mid-Pacific trough was somewhat less organized and possessed a reduced NE-SW tilt. Momentum fluxes over the subtropical belt were at a minimum during day 50-54.

At 700 mb (not shown for brevity), the cyclonic centre over India shifted about 5°-10° northwards. Easterlies between about 20°N and 30°N were thereby replaced by westerlies, while northwesterlies intensified over Arabia. The monsoon trough over southeast Asia was disrupted by the development of a well defined 700 mb ridge which extended from Japan to the Sumatra region and lay beneath the 200 mb trough [Over this region Ramamurthy (1969) noted what he termed as the southward shift of the lower tropospheric anticyclonic axis during severe "break" monsoon]. Adjacent to this ridge, a pronounced 700 mb trough formed directly under the anomalous 200 mb anticyclone over Guam.

Pronounced changes took place in the 200 mb divergent circulations (Fig. 13, bottom). The χ minimum centre normally located around 15°N, 125°E (*see* Fig. 1, bottom) moved to around 30°N-35°N, 90°E over Tibet [Daily horizontal distributions of χ show that this shift began around day 44 and proceeded as follows : day 44 (12·4°N, 125°E), 46 (17·2°N, 105°E), 48 (21·9°N, 100°E), 50 (28°N, 90°E), 52 (32°N, 85°E) and 54 (30°N, 95°E)]. Over the Philippines (15°N, 125°E), χ values became positive, and the strong divergent outflow which characterizes this region was replaced by convergent inflow and sinking motion. The χ component winds over India changes from easterly to strong northerly. Concurrently, upper level, E-W oriented divergent outflow was excited over tropical western Pacific with dominant centres at about 15°N, 165°E and 10°S, 170°E†. As will be shown later, these were also zones of unusual convective activity and, of course, upper air divergence. In addition, the χ minimum centre over the Caribbean Sea area shifted north by about 10°-15°.

Changes in the local Hadley circulations inevitably affect the mean meridional Hadley cell. During the abnormal period day 50-54, divergent southerlies were replaced by strong northerlies, between about 15°N and 35°N, over the monsoon region and to a lesser degree the Mexico-Caribbean Sea. Thus the northern hemisphere branch of the mean Hadley circulation was disturbed, and northerly $\bar{v}$ winds (not shown) covered nearly the entire domain under study. This intensification of northerly $\bar{v}$ winds, contributed to the easterly acceleration (westerly deceleration) of the northern hemisphere zonal winds over the tropical (mid-latitude) region.

Parallel changes occurred in the fields of divergence and cloudiness (Fig. 14). Over the Indian-southeast Asian region, the dominant divergence centre shifted over Tibet. Similarly the cloudiness maximum centre was displaced northward to about 25°N or beyond. Near the Philippines, upper convergence was associated with below season mean cloudiness. Anomalous upper divergence and cloudiness maxima that appeared in the western tropical Pacific around 15°N, 150°E and 10°S, 170°E, nearly coincided with abnormal upper (lower) tropospheric anticyclonic (cyclonic) circulations. In addition, over and to the north of the Gulf of Mexico, large 200 mb divergence and cloudiness zones developed.

†200 mb composite maps of tropical k maxima when compared with 200 mb composite maps of tropical k minima revealed similar tendencies. Divergent outflow from the tropical western Pacific was stronger during maxima than during minima.

8. Concluding remarks

Evidence has been presented that for the purpose of this study NMC wind data adequately describes some of the characteristic features of the tropospheric circulation fluctuations that occurred during the northern summer of 1970.

Around 12 July, abnormal transitions occurred culminating between 20 and 24 July in a circulation phase with singularly anomalous traits. This period was characterized by the following :

(1) 200 mb eddy kinetic energy at all latitudes and 700 mb kinetic energy in the tropics, decreased together to well below normal values, while upper tropospheric tropical zonal mean kinetic energy reached a maximum.

(2) Tropical baroclinic activity as measured by $\overline{c'^2}$ reached a minimum.

(3) The maximum cloudiness zone over the monsoon region shifted northwards to the Tibetan area, while dry weather and upper tropospheric convergent inflow prevailed, over southeast Asia and the Philippines.

(4) Convective activity and 200 mb divergence were abnormally enhanced as upper (lower) tropospheric anticyclonic (cyclonic) circulations developed over the tropical western North and western South Pacific.

(5) Western and central Pacific equatorial upper easterlies were unusually strong.

(6) The anticyclonic circulation over the Mexican area reached maximum intensity and maximum north latitude.

In summary, "break monsoon" conditions over India appear to be accompanied by wide-ranging coherent tropospheric changes. It is therefore of crucial importance that summer MONEX covers both regional and much larger scales, with an adequate observational system to revolve changes in the large-scale monsoonal flows to which regional variations are related.

We emphasize that our results should be treated as preliminary until other years are similarly examined. The summer circulation may differ from one year to another. This possibility is being examined using NMC data for the summers of 1969, 1971 and 1972; results will be reported later.

Acknowledgements

We are indebted to Mr. T. Gray of the Meteorological Satellite Laboratory, NOAA, for providing NMC wind data for this study. Professor J.C. Sadler of the University of Hawaii is gratefully acknowledged for the use of his satellite cloudiness data. We thank Dr. C.S. Ramage for his careful review of the manuscript. We also wish to thank Mrs. S. Arita for typing the manuscript.

This research has been supported by the Global Atmospheric Research Program, Climate Dynamic Research Section, National Science Foundation, under Grant No. ATM76-02502.

REFERENCES

Atkinson, G. D. and Sadler, J. C. 1970 Mean cloudiness and gradient-level wind charts over the tropics: Vol. I, Data. Tech. Rep. 215, U.S. Air Weather Service, 48 pp.

Colton, D. E. 1973 *J. atmos. Sci.*, **30**, pp. 1287-1302.

Holton, J. R. 1971 *Ibid.*, **29**, pp. 368-375.

Holton, J. R. and Colton, D. E. 1972 *Ibid.*, **29**, pp. 1124-1128.

Kanamitsu, N., Krishnamurti, T. N. and Depradine, C. 1972 *Ibid.*, **29**, pp. 698-706.

Krishnamurti, T. N. 1971(a) *J. appl. Met.*, **10**, pp. 1066-1096.

1971(b) *J. atmos. Sci.*, **28**, pp. 1342-1347.

REFERENCES (contd)

Krishnamurti, T. N. and Bhalme, H. N.	1976	*J. atmos. Sci.*, **33**, pp. 1937-1954.
Manabe, S., Holloway, Jr. J. L. and Stone, H. M.	1970	*Ibid.*, **27**, pp. 580-613.
Manabe, S., Hahn, D. C. and Holloway, Jr. J. L.	1974	*Ibid.*, **31**, 43-83.
Murakami, T.	1974	*Ibid.*, **31**, pp. 340-357.
	1976	*J. met. Soc. Japan*, **54**, pp. 175-181.
Murakami, T. and Frydrych, M.	1974	*J. atmos. Sci.*, **31**, pp. 1549-1555.
Murakami, T. and Unninayar, M. S.	1976	Changes in atmospheric circulations during the northern hemisphere winter (submitted to *Mon. Weath. Rev.*).
Oort, A. H. and Rasmusson, E. M.	1971	Atmospheric circulation statistics NOAA Professional Paper No. 5, Rockville, Md., 323 pp.
Ramage, C. S. and Raman, C. R. V.	1972	*Meteorological Atlas of the International Indian Ocean Expedition*, Vol. 2, Upper Air, National Science Foundation, Washington, D. C., 121. pp
Ramamurthy, K.	1969	Some aspects of the break in the Indian southwest monsoon during July and August. Forecasting Manual No. IV-18·3. Published by India met. Dep., 57 pp.
Sadler, J. C.	1967	The tropical upper tropospheric trough as a secondary source of typhoons and a primary source of trade wind disturbances. AFCRL-67-0203 Contract No. AF 19 (628)-3860, Hawaii Ins. Geophys. Univ. Hawaii, HIG-67-12.
	1968	Average cloudiness in the tropics from satellite observations, International Indian Ocean Expedition Met. Monogr. No. 2, East-West Center Press, Univ. of Hawaii, 22 pp.
	1975(a)	The upper tropospheric circulation over the global tropics. Tech. Rep., Grant No. GA-36301, Department of Meteorology, Univ. Hawaii, 35 pp.
	1975(b)	Tropical cyclone initiation by the tropical upper tropospheric trough. Tech. Rep., Naval Environmental Prediction Research Facility, Monterey, California, 33 pp.
Saltzman, B.	1957	*J. Met.*, **14**, pp. 425-431.
	1970	*Rev. Geophys.*, **8**, pp. 289-302.
Saltzman, B. and Teweles, S.	1964	*Tellus*, **16**, pp. 432-435.
Webster, P. J.	1972	*Mon. Weath. Rev.*, **100**, pp. 518-541.
Webster, P. J. and Keller, J. L.	1975	*J. atmos. Sci.*, **32**, pp. 1283-1300.
Washington, W. M. and Daggupaty, S. M.	1975	*Mon. Weath. Rev.*, **103**, pp. 105-114.